The Formation of Covalent Adducts between Benzo[a]pyrenediol Epoxide and RNA: Structural Analysis by Mass Spectrometry†

JoAnn Yamamoto,‡ Raj Subramaniam,§ Alan R. Wolfe, and Thomas Meehan*
Division of Toxicology and Department of Pharmacy, School of Pharmacy, University of California, San Francisco, California 94143

Received August 29, 1989; Revised Manuscript Received December 26, 1989

ABSTRACT: Racemic 7-*r*,8-*t*-dihydroxy-9-*t*,10-*t*-epoxy-7,8,9,10-tetrahydrobenzo[*a*]pyrene was reacted with yeast RNA. Modified nucleosides were isolated and resolved by high-performance liquid chromatography; nine adduct peaks were collected for analysis. The bases in these adducts were identified by comparing their retention times with those of adducts from poly(G), poly(A), and poly(C). These samples gave two major and two minor Guo adducts, four major Ado adducts, and at least four Cyd adducts. The relative efficiencies of adduct formation with the polyribonucleotides were poly(G) > yeast RNA > poly(A) > poly(C). Fluorescence measurements show that emission from Guo adducts is strongly quenched relative to that from Ado adducts. Liquid secondary ion mass spectrometry (LSIMS) of underivatized samples and electron-impact mass spectrometry (EIMS) of permethyl derivatives were used to confirm the base identities and establish the alkylation sites of the RNA adducts. Unique nitrogen-containing hydrocarbon fragments that were observed with all samples by EIMS establish that in each adduct analyzed the C-10 position of the hydrocarbon is linked to the exocyclic amino group of the base. This suggested that the multiple adducts formed with each base are diastereomers derived from cis/trans epoxide ring opening of the (+) and (−) enantiomers of the carcinogen. Several adducts exhibited molecular ions by both LSIMS and EIMS. Large fragments observed by EIMS usually resulted from the loss of CH_3OH, $CH_3O^{\bullet}$, CH_2O, $CH_3^{\bullet}$, and $H^{\bullet}$ from the molecular ion. Major fragmentation pathways also resulted in formation of nucleoside, base, ribose, hydrocarbon, and base–hydrocarbon ions. Each of these major ions in turn resulted in further characteristic fragmentation patterns.

Benzo[*a*]pyrene (BP)[1] is a potent inducer of tumors in animals and a suspected cause of human cancer which occurs widely as an environmental contaminant. It is a procarcinogen; i.e., it must be metabolized to an electrophilic active form in order to exhibit biological activity (Heidelberger, 1975; Brookes & Lawley, 1964; Gelboin, 1969). The principal activated form of BP (Scheme I) is 7-*r*,8-*t*-dihydroxy-9-*t*,10-*t*-epoxy-7,8,9,10-tetrahydrobenzo[*a*]pyrene, or *anti*-BPDE

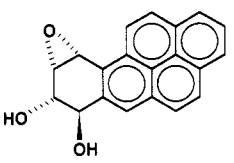

(+)-*anti*-BPDE

(Sims, et al., 1974; Huberman et al., 1976; Meehan et al., 1976; Weinstein et al., 1976; Koreeda et al., 1976; King et al., 1976); the 7r,8t,9c,10c isomer of BPDE (*syn*-BPDE) is also generated. All four possible diastereomers of *syn*- and *anti*-BPDE are formed in mammalian cells (Ivanovic et al., 1978); the most mutagenic and carcinogenic of these is the 7*R* or (+) enantiomer of *anti*-BPDE (Wood et al., 1977; Buening et al., 1978). Like most chemical carcinogens, BPDE alkylates nucleic acids, proteins, and other cellular nucleophiles; the DNA adducts are believed to initiate carcinogenesis (Miller & Miller, 1972; Heidelberger, 1975; McCann & Ames, 1976).

The primary alkylation target of BPDE in DNA and RNA both in vivo and in vitro is the N^2 position of guanine, which is linked to C-10 of the hydrocarbon (Koreeda et al., 1976; King et al., 1976; Jeffrey et al., 1976; Straub et al., 1977). Other BPDE–DNA adducts have been reported to involve alkylation at N^6 of adenine (Straub et al., 1977; Jeffrey et al., 1979) and N-7 of guanine (Osborne et al., 1978, 1981). The N-7 guanine adduct is unstable and thus has not been characterized in detail. Some evidence supports adduct formation at O-6 of guanine (Osborne et al., 1981) and N^4 of cystosine (Meehan et al., 1977; Straub et al., 1977). The alkylation site on cytosine has not been definitively established.

Direct structural analysis of covalent adducts formed between polycyclic aromatic hydrocarbons and nucleic acids has been carried out in only a limited number of cases, primarily due to the difficulty of preparing sufficient quantities of adducts. BPDE–poly(G) and BPDE–poly(A) adducts have been completely characterized by NMR and CD (Weinstein et al., 1976, Koreeda et al., 1976; Jeffrey et al., 1979). BPDE adducts of dGuo, dAdo, and dCyd from DNA have been analyzed by high-resolution mass spectrometry (Straub et al., 1977).

Because of their postulated involvement in tumor initiation, DNA adducts have been the focus of attention in carcinogenesis research. BPDE–RNA adducts have only been

† This work was supported in part by grants from the National Cancer Institute (CA 40598) and the Elsa U. Pardee Foundation.

‡ Present address: Abbott Laboratories, Abbott Park, North Chicago, IL 60064.
§ Present address: nanoFilm Corp., 14675 Foltz Industrial Pkwy., Strongsville, OH 44136.

[1] Abbreviations: BP, benzo[*a*]pyrene; (±)-*anti*-BPDE, racemic 7-*r*,8-*t*-dihydroxy-9-*t*,10-*t*-epoxy-7,8,9,10-tetrahydrobenzo[*a*]pyrene; B, base; R, ribose; LSIMS, liquid secondary ion mass spectrometry; EIMS, electron-impact mass spectrometry; BPT, fragment corresponding to 7,8,9-trihydroxy-7,8,9-trihydrobenzo[*a*]pyrene radical; HPLC, high-performance liquid chromatography; *cis*- and *trans*-tetrol, (±)-7-*r*,8-*t*,9-*t*,10-*t*- and (±)-7-*r*,8-*t*,9-*t*,10-*c*-tetrahydroxy-7,8,9,10-tetrahydrobenzo[*a*]pyrene, respectively.

0006-2960/90/0429-3966$02.50/0

identified on the basis of chromatographic comparisons with adducts from synthetic polyribonucleotides or monomeric ribonucleosides. Carcinogen–RNA adducts are deserving of study for several reasons, however. RNA adducts may have a role in the cellular damage caused by carcinogens; furthermore, in some cases, RNA may be a useful model for DNA in the study of carcinogen–nucleic acid adduct formation. In this paper we report the structures of covalent adducts formed in vitro between racemic *anti*-BPDE and yeast RNA as determined by secondary ion and electron-impact mass spectrometry.

Experimental Procedures

Chemicals and Supplies. Yeast RNA, poly(G), poly(A), poly(C), calf thymus DNA, DNase II, phosphodiesterase II, and alkaline phosphatase were obtained commercially. The preparation of (±)-*anti*-BPDE and (±)-*anti*-[G-^{3}H]BPDE have been reported (Harvey & Fu, 1978; Meehan & Straub, 1979). (+)- and (−)-*anti*-[1-^{3}H]BPDE were obtained from NCI and were diluted with unlabeled (+)- and (−)-*anti*-BPDE prepared as described by Yagi et al. (1977b) to about 3 mCi/mmol. All other chemicals were at least reagent grade quality. C_{18} reverse-phase Sep-Pak cartridges were obtained from Waters Associates.

Formation of BPDE–RNA Adducts and Removal of Noncovalently Bound Hydrocarbon. Adducts between the carcinogenic epoxide and polyribonucleotides were generated in mixtures containing 0.01 M potassium phosphate (pH 7.5), 1 mg/mL nucleic acid, labeled or unlabeled (±)-*anti*-BPDE (12 nmol/mg of nucleic acid), and 3% acetone (by volume). The reaction was started by the addition of (±)-*anti*-BPDE (in acetone), and the samples were incubated at room temperature for 3 h. At the end of the incubation period the polynucleotide sample was extracted three times with 3 volumes of water-saturated ethyl acetate, in order to remove physically bound tetrols (the hydrolysis products of *anti*-BPDE). The samples were heated to 75 °C for several minutes between extractions to facilitate hydrocarbon removal. The aqueous phase was transferred to 16-mm (dry cylindrical diameter) Spectrapor 4 cellulose dialysis tubing (M_r cutoff 12000–14000). The tubing was prewashed with a dilute DNA solution and rinsed with distilled water. Dialysis was carried out at 4 °C against 2 L of 0.01 M potassium phosphate (pH 7.5) for 69 h. The dialysate was changed at 20 and 45 h. After dialysis, the samples were brought to 0.1 M sodium chloride and the nucleic acid was precipitated by the addition of 2.5 volumes of cold ethanol. After centrifugation, the pellet was dried with a stream of nitrogen.

Hydrolysis of Phosphodiester Backbone of BPDE-Modified RNA. Modified polyribonucleotides were dissolved in 0.3 N KOH at a concentration of 1 mg of RNA/mL. The samples were heated in a boiling water bath for 15 min; after cooling, the solution was brought to 0.1 M in glycine and 1 mM in magnesium chloride and zinc chloride, and the pH was adjusted with HCl to ~10. Nucleotides were converted to nucleosides by incubating samples with alkaline phosphatase (50 units/mg of polynucleotide) for 21 h at 37 °C. After 6 h, an additional 20 units of alkaline phosphatase/mg of nucleic acid was added.

Isolation of Adducts. Modified nucleosides were separated from unmodified nucleosides in the nucleic acid digests with C_{18} Sep-Pak cartridges. After loading the aqueous samples onto the Sep-Pak, the cartridge was washed with water to remove unmodified nucleosides and the *anti*-BPDE nucleoside adducts were eluted with methanol. The samples were concentrated with a stream of nitrogen. The mixture of modified nucleosides was resolved into individual adducts by reverse-phase HPLC using a Du Pont C_{18} column (Zorbax ODS; 4.6 mm × 25 cm). Samples were eluted isocratically with 50% methanol/water (previously mixed and degassed) at a flow rate of 0.7 mL/min and detected by fluorescence. Excitation was at 245 nm, and emission was measured at wavelengths >320 nm by using a cutoff filter. Adduct fractions collected from the HPLC eluate were further purified by TLC prior to mass spectrometry. Adduct samples stored for more than a few weeks were kept at −80 °C.

Thin-Layer Chromatography of Adducts. TLC was performed by using 250-μm Analtech silica gel GF plates (2.5 × 10 cm). Triethylamine was prespotted along the origin and dried to inhibit adduct breakdown. The adduct sample was streaked onto the plate and dried with a hot air blower. The plate was developed in *n*-hexane, dried, and developed in acetone, a procedure that did not significantly move the adducts. The plates were wet with ethanol, and the area near the origin was scraped off. The adducts were extracted from silica by vortexing in 10 mL of 70% acetone/water, with one drop of triethylamine. The silica suspension was centrifuged and the supernatant filtered (0.45 μm, Millipore), evaporated under a stream of nitrogen, and redissolved in methanol.

Adduct Permethylation. BPDE–RNA adducts were permethylated by using a method adapted from the procedures of Hakomori (1964) and Sjöberg (1966). NaH (0.95 g in a 60% oil dispersion) was washed six to eight times with HPLC-grade petroleum ether. After each washing, the ether phase was decanted, leaving a thin film of ether above the NaH. The solid residue was dried under a stream of argon, and 10 mL of dimethyl sulfoxide (distilled over CaH_2) was added. The resulting suspension was sonicated under argon for 10 min with a Branson Model 52 sonicator at low power (20–40 W). This methanesulfinyl carbanion solution was stored under argon in a desiccator at −80 °C until needed and centrifuged before use. Samples containing 10–20 μg of adduct were evaporated under a stream of argon and stored overnight at 4 °C under P_2O_5 before use. In the methylation reaction (performed under argon) an adduct sample was first dissolved in 40 μL of dry, redistilled dimethyl sulfoxide; 5 μL of methanesulfinyl carbanion solution was added, and the mixture was vortexed for 30 s. Methyl iodide (2 μL) was added followed by 60 s of vortexing. One milliliter of water was then added to stop the reaction. The permethylated adducts were extracted into 1 mL of $CHCl_3$, which was washed four times with 1 mL of water. The adduct solution was transferred to capillary tubes and evaporated under argon in preparation for EIMS.

Mass Spectrometry. Liquid secondary ion mass spectrometry was carried out with underivatized samples in a thioglycerol or glycerol matrix on a Kratos MS50 equipped with a cesium gun. Electron-impact mass spectrometry was performed on permethylated *anti*-BPDE–nucleoside adducts. Samples were introduced into the mass spectrometer by direct probe insertion.

Instruments. Radioactivity was measured with a Beckman LS-9000 liquid scintillation counter using Aquasol-2 (New England Nuclear), and dpm were obtained by automatic quench monitoring with an external standard. Absorbance spectra were obtained with a Cary 118 or an Aminco DW-2a double-beam spectrophotometer. A Kratos LC fluorometer (Model FS-970) was used to monitor adduct elution during HPLC.

Results and Discussion

The efficiency with which BPDE alkylates the polyribo-

Table I: Modification Levels of Polyribonucleotides[a]

polynucleotide	hydrocarbons/base		
	reaction mixture (A)	product (B)	B/A[b]
poly(G)	1/2750	1/10600	0.26
poly(A)	1/58	1/1100	0.053
poly(C)	1/62	1/4700	0.013
yeast RNA	1/30	1/500	0.06

[a] BPDE was reacted with yeast RNA and synthetic polyribonucleotides. The ratios of hydrocarbons per base in the reaction mixture and product (modified polynucleotide) are indicated. [b] The fraction of added BPDE recovered as adducts.

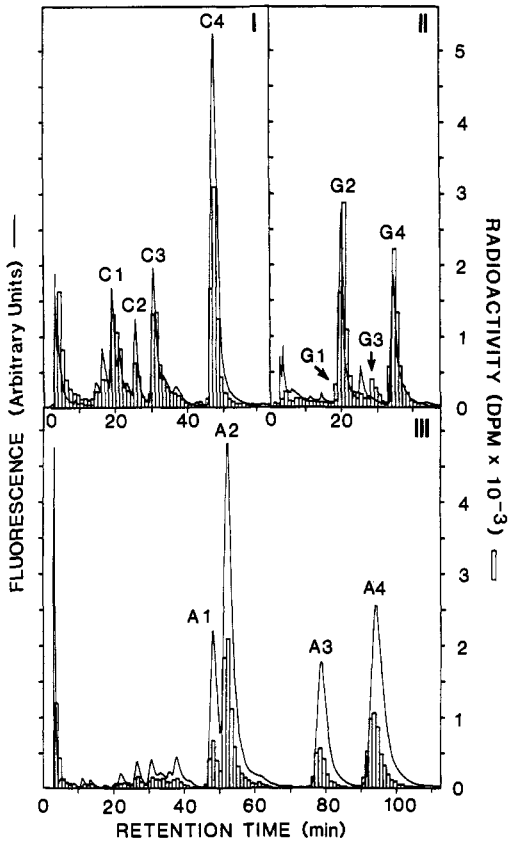

FIGURE 1: HPLC elution profiles of covalent adducts between (±)-*anti*-BPDE and synthetic polyribonucleotides. Racemic [^{3}H]-BPDE was reacted with poly(C) (I), poly(G) (II), and poly(A) (III). The adducts were isolated and resolved by reverse-phase HPLC as described under Experimental Procedures and detected by fluorescence (——) or tritium content (□). Four major adducts were obtained from both poly(C) and poly(A), and two major and two minor adducts were obtained with poly(G). The minor adduct G1 is not resolved from G2 in the chromatogram shown.

nucleotides tested varies widely. Because the nucleic acid used was present in large excess, the extent of adduct formation is a linear function of the initial BPDE concentration. The ratio of BPDE to bases in the initial reaction mixture and the ratio of adducts to bases in the polynucleotide after reaction and removal of noncovalently bound tetrols are given in Table I. The efficiency of alkylation is given by the ratio of hydrocarbons in the product to those in the reaction mixture (last column, Table I). Poly(G) is alkylated most, followed by yeast RNA, poly(A) and poly(C). There is a 20-fold difference in reaction efficiency between poly(G) and poly(C). In all cases, the bulk of the added BPDE hydrolyzes to *trans*- and *cis*-tetrols, a reaction catalyzed by nucleic acids (Geacintov et al., 1984).

HPLC adduct profiles from the reaction of (±)-*anti*-[^{3}H]BPDE with poly(C), poly(G), and poly(A), respectively,

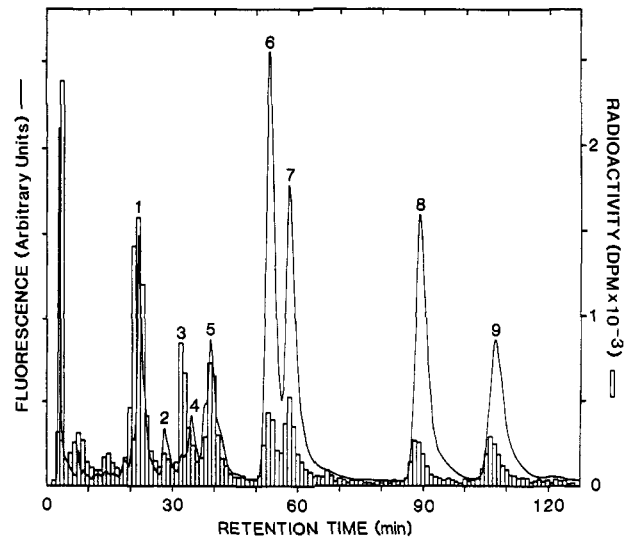

FIGURE 2: BPDE adducts from yeast RNA. Adducts were isolated and analyzed as in Figure 1. At least nine peaks were resolved. Adducts C1, G1, and G2 coelute as peak 1 (G2 is the primary component). Peak 2 consists of adduct C2 and *trans*-tetrol. Peak 3 is adduct G3, which is partially resolved from adduct C3 in peak 4. Peak 5 represents adduct G4. Peak 6 is primarily adduct A1, with adduct C4 coeluting. Peaks 7, 8, and 9 are adducts A2, A3, and A4, respectively.

are shown in Figure 1. At least four poly(C) adducts were resolved. Two major adducts (peaks G2 and G4) are formed by reaction of the hydrocarbon with poly(G) and correspond to trans addition of the 7*S* and 7*R* enantiomers of BPDE, respectively, to the exocyclic amino group of guanine, forming a set of resolvable diastereomers (Weinstein et al., 1976; Nakanishi et al., 1977; Meehan & Straub, 1979; Panthananickal & Marnett, 1981). Poly(G) adducts formed by cis addition of N^2-guanine to (+)- and (−)-*anti*-BPDE also occur. We obtained a minor adduct (G3, Figure 1) which has the relative retention time expected for the cis adduct of (−)-BPDE. However, the cis (+)-*anti*-BPDE–Guo adduct (G1) elutes close to the trans (−)-BPDE–Guo adduct (G2) and so was only observed when resolved (+)-*anti*-BPDE was used separately (results not shown). The ratio of peak areas of the major (+) and (−) Guo adduct peaks (G4/G2) is roughly 1:1; i.e., the binding of (±)-*anti*-BPDE to poly(G) is not enantioselective. This is in contrast to the binding of *anti*-BPDE to duplex DNA, where reaction by the (+) enantiomer of BPDE is strongly favored (Meehan & Straub, 1979). Four adducts are formed with poly(A); peaks A1–A4 correspond to the trans (+)-, cis (−)-, trans (−)-, and cis (+)-BPDE–Ado adducts, respectively (Jeffrey et al., 1979).

An HPLC profile of the nucleoside adducts obtained from the reaction of (±)-*anti*-[^{3}H]BPDE and yeast RNA is shown in Figure 2. Nine peaks were resolved; comparison of retention times with the chromatograms in Figure 1 suggests that peaks 1, 3, and 5 are Guo adducts, peaks 6–9 are Ado adducts, and peaks 2 and 4 are Cyd adducts. In addition, Cyd adducts would be expected to coelute with peaks 1 and 5, and *trans*-tetrol with peak 2. The elution profile is quite similar to that obtained with BPDE adducts from calf thymus DNA (Meehan & Straub, 1979). However, the Ado adducts represent a higher proportion of total RNA adducts (34%) than the fraction of dAdo adducts we obtained from native or denatured DNA (6% or 16% respectively; data not shown). Relative to the homopolymers, the yeast RNA adduct profile exhibits more cis Guo adducts and more trans Ado adducts.

The chromatograms in Figures 1 and 2 reveal that the fluorescence yields of BPDE–ribonucleoside adducts vary

Table II: Fragments Observed by Liquid Secondary Ion Mass Spectrometry[a]

sample	m/z	fragment composition
1	587 $M^+ + 2$	$[BPT\cdot Guo + 2]^+$
	454 $M^+ + 2 - R$	$[BPT\cdot Gua + 2]^+$
	149 $M^+ - BPT - R$	Gua^+
1A	645 $M^+ - 2 + Na + K$	$[BPT\cdot Guo - 2 + Na + K]^+$
	629 $M^+ - 2 + 2Na$	$[BPT\cdot Guo - 2 + 2Na]^+$
2		
3	587 $M^+ + 2$	$[BPT\cdot Guo + 2]^+$
	454 $M^+ + 2 - R$	$[BPT\cdot Gua + 2]^+$
	149 $M^+ - BPT - R$	Gua^+
4	587 $M^+ + 2$	$[BPT\cdot Guo + 2]^+$
	454 $M^+ + 2 - R$	$[BPT\cdot Gua + 2]^+$
	149 $M^+ - BPT - R$	Gua^+
	545 M^+	$[BPT\cdot Cyd]^+$
	413 $[M + 1]^+ - R$	$[BPT\cdot Cyt + 1]^+$
5	587 $M^+ + 2$	$[BPT\cdot Guo + 2]^+$
6		
7	570 $[M + 1]^+$	$[BPT\cdot Ado + 1]^+$
8	570 $[M + 1]^+$	$[BPT\cdot Ado + 1]^+$
9	570 $[M + 1]^+$	$[BPT\cdot Ado + 1]^+$

[a] BPDE·RNA adducts were generated as described under Experimental Procedures. The modified RNA was chemically hydrolyzed, and nine adduct fractions were isolated by HPLC. Sample numbers correspond to the peaks in Figure 2. Each sample (except 1A) was subjected to further purification by silica thin-layer chromatography.

considerably, depending on the identity of the base and the stereochemistry of the adduct. The emission from Guo adducts is quenched, being 25% or less than that of tetrol (data not shown). Ado adducts exhibit much stronger emission, from 1.25 to 3 times that of tetrol. The fluorescence yields of Cyd adducts (based on limited data) appear to be intermediate. The pattern of fluorescence yields of BPDE–deoxyribonucleoside adducts is similar. The pyrenyl residue is the predominant fluorophore in these nucleoside adducts; apparently, the Ado and Guo residues interact with it in markedly different ways. This variation may result from differences in conformation or intramolecular dynamics. A comparable pattern of purine effects on quantum yields has been noted in model compounds in which an acridine derivative is linked to a base (at N-9) via a polymethylenic chain (Constant et al., 1988). When BP fluorescence is quenched by free nucleosides in water/ethanol solution, the effects of dGuo and dAdo are similar (Geacintov et al., 1976).

About 25 μg of each of the major RNA adducts was isolated by collecting fractions. The samples were further purified by TLC and analyzed by LSIMS (results are summarized in Table II). LSIMS provides a fast and simple method for the identification of the bases in DNA or RNA that react with chemical carcinogens. The technique is sensitive and requires a minimum of sample preparation. The limitation is that this approach provides little structural detail. LSIMS of the unmethylated samples gave molecular ions in all cases where a spectrum was obtained.

The sample from peak 1 exhibited an ion at m/z 587, corresponding to a BPDE–Guo adduct, as well as ions representing BPDE–Guo minus ribose, and the base guanine. Peaks 3 and 5 gave the same ions, indicating that they too were BPDE–Guo adducts. With sample 1A the TLC purification step was omitted; it exhibits ions at m/z 645 and 629 due to associated cations. Peak 4 contained both Guo and Cyd adducts; ions at m/z 545 and 413 represent BPDE–Cyd and BPDE–Cyd minus ribose. Peaks 7–9 were identical by LSIMS and exhibited the ion representing BPDE–Ado plus a proton (m/z 570). Peak 2 did not yield sufficient material for analysis. We also failed to obtain an LSI mass spectrum for peak 6, possibly due to losses during purification or instrumental problems.

To obtain more information, a portion of each sample was permethylated and analyzed by EIMS. Tables III and IV present representative spectra from peaks 1, 8, 2, and 4. Samples representing adducts with the same base (Guo in peaks 1, 3, and 5 and Ado in peaks 7–9) gave essentially identical spectra. The molecular ion (M^+) in the EI spectrum was usually weak. Various ions closely related to M^+ were observed. von Minden and McCloskey (1973) have proposed a fragmentation pattern involving the methoxy groups of the sugar for permethylated free nucleosides. We would expect similar losses from the hydrocarbon and loss of methyl groups

Table III: Representative Molecular Ion Related Fragments from the Electron-Impact Mass Spectra of Permethyl BPDE–RNA Adducts

	sample		
proposed fragment ion	Guo, peak 1, m/z (% rel abundance)	Ado, peak 8, m/z (%)	Cyd, peak 2, m/z (%)
M^+ or $[M + 1]^+$	698 (0.9)	667 (1.3)	
$[M + 1]^+ - CH_2O$	668 (0.9)		
$M^+ - CH_3OH$	665 (1.5)	635 (4)	
$[M \text{ or } M + 1]^+ - CH_3OH - CH_3^\cdot$	650 (1.2), 651 (1.3)	620 (2.4)	
$M^+ + C_2H_6O - 3CH_3OH$			593 (1.6)
$[M \text{ or } M + 1]^+ - CH_3OH - CH_3O^\cdot$	634 (8)	604 (22), 605 (8)	
$M^+ - 2 - 2CH_3OH$			577 (0.8)
$M^+ - CH_3OH - CH_2O - CH_3^\cdot$		590 (1.5)	
$[M \text{ or } M + 1]^+ - 2CH_2O - CH_3O^\cdot$	607 (0.9)	576 (1)	
$[M \text{ or } M + 1]^+ - 2CH_3OH - CH_2O - CH_3^\cdot$	588 (0.9), 589 (1)		534 (1.8), 535 (2.3)
$M^+ - 3CH_2O - CH_3O^\cdot$	576 (1.9)		522 (1.8)
$[M \text{ or } M + 1]^+ - 2CH_3OH - 2CH_2O$			519 (9), 520 (5)
$M^+ - 3CH_2O - CH_3^\cdot - CO$	564 (1.4)	534 (1.7)	
$[M + 1]^+ - 4CH_2O - CH_3^\cdot$	563 (1.5)		
$[M + 1]^+ - 2CH_3OH - 2CH_2O - CH_3^\cdot$			505 (5)
$[M + 1]^+ - 3CH_3OH - CH_2O - CH_3^\cdot$			503 (9)
$[M \text{ or } M + 1]^+ - 4CH_2O - CO$	549 (1.3)	519 (5), 520 (3)	
$M^+ - 2CH_3OH - 3CH_2O$			489 (3)
$[M + 1]^+ - 4CH_2O - CH_3^\cdot - CO$	535 (2.3)	505 (1.7)	
$[M + 1]^+ - 5CH_2O - CH_3^\cdot$	533 (1.4)	503 (5)	
$[M + 1]^+ - 2CH_3OH - 3CH_2O - CH_3^\cdot$			475 (3)
$[M \text{ or } M + 1]^+ - 5CH_2O - CO$	520 (8)	489 (2.3)	
$M^+ - CH_3OH - 5CH_2O$			461 (3)
$M^+ - 5CH_2O - CH_3^\cdot - CO$	504 (5)		
$[M + 1]^+ - 6CH_2O - CH_3^\cdot$	503 (9)		
$M^+ - CH_3OH - 5CH_2O - CH_3^\cdot$			446 (27)
$[M + 1]^+ - 2CH_3OH - 4CH_2O - CH_3^\cdot$			445 (55)

Table IV: High-Mass Ions from the Electron-Impact Mass Spectrum of Permethyl BPDE–RNA Peak 4[a]

m/z (% rel abundance)	proposed fragment ion		
	Guo adduct		Cyd adduct
643 (1.4)			M^+
635 (2.2)	$M^+ - CH_3OH - CH_2O$		
611 (2.1)			$M^+ - CH_3OH$
597 (1.7)			$[M + 1]^+ - CH_3OH - CH_3^\bullet$
588 (1.5)	$M^+ - 2CH_3OH - CH_2O - CH_3^\bullet$		
580 (13)			$M^+ - CH_3OH - CH_3O^\bullet$
519 (3.5)			$M^+ - 2CH_3OH - 2CH_2O$
504 (4)	$M^+ - 5CH_2O - CH_3^\bullet - CO$		
461 (4)	$[M + 1]^+ - R - CH_3OH - CH_2O$	or	$M^+ - CH_3OH - 5CH_2O$
445 (25)	$M^+ - R^b - CH_3OH - CH_2O - CH_3^\bullet$	or	$[M + 1]^+ - 2CH_3OH - 4CH_2O - CH_3^\bullet$

[a] This fraction contains Guo adducts due to overlap with peak 3 (see Figure 2). [b] R = ribose moiety.

Scheme I: Major Fragmentation Pathways of Permethyl BPDE–RNA Adducts[a]

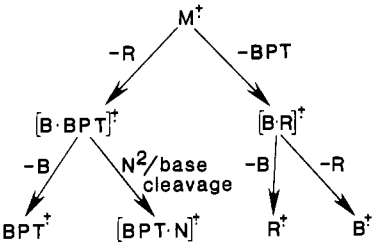

[a] M^+ is the molecular ion, B^+ the base ion, and R^+ the sugar ion. BPT^+ is the hydrocarbon ion, generated by scission of the bond between the base and C-10 of the hydrocarbon. Cleavage between the exocyclic amino group of the base (N^2 in guanine, N^6 in adenine, and N^4 in cytosine) and its adjacent ring carbon gives $[BPT{\cdot}N(CH_3)]^+$.

from the bases. Each of these types of ions was observed in all of our samples.

General Fragmentation Pattern. The major fragmentation pathways of the permethylated adducts are illustrated in Scheme I. Major ions are the base (B) linked to the hydrocarbon (BPT), designated $[B{\cdot}BPT]^+$, generated by loss of ribose (R); B plus R, designated $[B{\cdot}R]^+$, generated by loss of the hydrocarbon; BPT^+ obtained by loss of R and B; R^+ generated by loss of BPT and B; B^+ generated from loss of BPT and R; and $[BPT{\cdot}N(CH_3)]^+$ generated by cleavage of the bond between the exocyclic amino groups and the C-2, C-6, or C-4 carbons of guanine, adenine, or cytosine, respectively.

The higher mass end of the spectra is dominated by fragment ions from the adduct that has lost ribose. The pattern is determined by the identity of the base and follows strictly that observed by von Minden and McCloskey (1973). In addition, some peaks from the fragmentation of the permethylated benzo[*a*]pyrene nucleus are present.

In the middle mass range (*m/z* 239–374) the fragmentation pattern is due to the hydrocarbon moiety. Two types of ions are observed. One set is generated by cleavage of the bond between the exocyclic amino group of the base and the hydrocarbon, and one set by cleavage between the amino group and the adjacent ring carbon of the base. The latter set of fragments are vital to identifying the alkylation sites on the bases. The fragmentation pattern of the hydrocarbon was described by Straub et al. (1977).

Ions in the lower mass range (*m/z* 45–175) are primarily due to the sugar moiety. These ions are of moderate intensity and follow the fragmentation pattern reported for nucleosides by von Minden and McCloskey (1973).

Table V: Fragment Ions from the Electron-Impact Mass Spectra of Permethyl BPDE–RNA Adducts Generated by Loss of Ribose (R)

proposed fragment ion	sample	
	Guo, peak 1, *m/z* (%)[a]	Ado, peak 8, *m/z* (%)[a]
$M^+ - 2 - R - CH_3^\bullet$		475 (6)
$M^+ - R - CH_3OH$	490 (2.4)	460 (11)
$[M \text{ or } M + 1]^+ - R - CH_3OH - CH_3^\bullet$	476 (2.3)	445 (42)
$[M \text{ or } M + 1]^+ - R - CH_3OH - CH_2O$	461 (4)	430 (30)
$M^+ - R - CH_3OH - CH_2O - CH_3^\bullet$	445 (50)	415 (10)
$[M + 1]^+ - R - 2CH_3OH - CH_2O$	429 (41)	
$[M + 1]^+ - R - CH_3OH - 2CH_2O$		401 (9)
$[M \text{ or } M + 1]^+ - R - CH_3OH - 2CH_2O - CH_3^\bullet$	415 (11)	386 (4)
$[M + 1]^+ - R - CH_3OH - 3CH_2O$	401 (12)	

[a] % relative abundance.

Molecular Ion Related EI Fragments. Table III presents the major fragment ions obtained in the EI mass spectra of permethylated peak 1 (a Guo adduct), peak 8 (an Ado adduct), and peak 2 (a Cyd adduct). Weak molecular ions were observed for samples 1 and 8. The Guo adduct exhibited a molecular ion at *m/z* 698 (relative abundance 0.88%), representing the uptake of eight methyl groups. The molecular ion for the Ado adduct occurred at *m/z* 667 (1.3% relative abundance), representing seven methylations. Various losses of CH_3OH, $CH_3O^\bullet$, and CH_2O lead to Guo adduct ions between *m/z* 504 and 668 and Ado adduct ions between 503 and 635. Although most of these ions are of low intensity, *m/z* 604 for the Ado adduct occurs with 22% relative abundance. This ion, $M^+ - CH_3OH - CH_3O^\bullet$, is unusually stable for its mass range and was consistently observed in the Ado adduct samples.

Due to the limited amount of material, the sample from peak 2 gave a very weak spectrum and did not exhibit a molecular ion. The highest mass ions at *m/z* 595 and 593 probably represent base-catalyzed ring opening of the ribose, followed by methylation at C-1′ and C-4′. Basic conditions would result from the presence of moisture during the methylation procedure. These $M^+ + C_2H_6O$ ions were also observed on two other occasions.

A molecular ion was observed for the Cyd adduct in sample 4, however; it occurs at *m/z* 643, representing the uptake of seven methyl groups. Related high-mass, low-abundance fragments are given in Table IV. EIMS also provided evidence for the presence of a second adduct in this sample. LSIMS and peak retention times indicate that this is a Guo adduct, presumably derived from overlap between peaks 3 and 4. Table IV lists several high-mass fragments for the Guo adduct; its molecular ion was not observed, probably due to its low abundance.

EI Fragment Ions of the Base with the Hydrocarbon Moiety. The EI fragment pattern we observe for the base carrying the permethylated hydrocarbon $[B{\cdot}BPT]^+$ is related to that observed for the base alone. Almost every base fragment ion corresponds to a set of adduct fragment ions generated by the loss of methyl or methoxy radicals from the hydrocarbon (see Table V). B^+, $[B + H]^+$, and $[B + 2H]^+$ ions were weak in all cases studied. $[B{\cdot}BPT]^+$ ions are intense compared to the molecular ion related fragments. Beginning with the loss of CH_3OH from $[M - R]^+$ (at *m/z* 490), the Guo adduct spectrum has ions every 15 mass units until *m/z* 401. The Ado adduct gives a similar sequence from $[M - R - 2]^+ - CH_3^\bullet$ at *m/z* 475 to 386.

Table VI: Representative $[BPT{\cdot}N(CH_3)]^+$ and Related Fragment Ions in the Electron-Impact Mass Spectra of Permethyl BPDE–RNA Adducts

	proposed hydrocarbon fragments from		
m/z	$[BPT{\cdot}N(CH_3)]^+$	BPT^+	tetrol
344	$[BPT{\cdot}N(CH_3)]^+ - CH_2O$	$BPT^+ - 1$	$[tetrol]^+ - CH_3OH$
341[a]	$[BPT{\cdot}N(CH_3) - 1]^+ - CH_3OH$		
313	$[BPT{\cdot}N(CH_3)]^+ - CH_3O^{\cdot} - CH_2O$	$BPT^+ - CH_3OH$	$[tetrol]^+ - CH_3OH - CH_3O^{\cdot}$
295[a]	$[BPT{\cdot}N(CH_3)]^+ - 2CH_3OH - CH_3^{\cdot}$		
269	$[BPT{\cdot}N(CH_3)]^+ - 3CH_2O - CH_3^{\cdot}$	$BPT^+ + 1 - CH_3OH - CH_2O - CH_3^{\cdot}$	$[tetrol]^+ - CH_3OH - 2CH_2O - CH_3^{\cdot}$
255	$[BPT{\cdot}N(CH_3)]^+ - 3CH_2O - NCH_3^{\cdot}$	$BPT^+ - 3CH_2O$	$[tetrol]^+ - 3CH_2O - CH_3O^{\cdot}$

[a] m/z unique to $[BPT{\cdot}N(CH_3)]^+$ fragment.

EI Fragment Ions of the Sugar. Simple cleavage of the glycosidic bond produces the sugar fragment (R^+, m/z 175), usually accompanied by $[R - H]^+$. R^+ can lose methanol, giving rise to a charge-stabilized ion (m/z 143). Loss of CO followed by hydrogen from this ion results in ions at m/z 115 and 114 (von Minden & McCloskey, 1973). Relatively high intensities are observed for the ion with three skeletal carbons carrying two methoxy groups (m/z 101). Simple cleavage of the C-4′,5′ bond in R or the m/z 143 or 101 fragments produces ions at m/z 129, 99, or 45, respectively. All the spectra recorded for the Guo, Ado, and Cyd adducts showed the pattern expected for ribose.

EI Fragment Ions from the Hydrocarbon. Two sets of hydrocarbon ions are observed, one containing nitrogen and one without. Epoxide ring opening preferentially occurs with formation of a C-10 benzylic carbonium ion (Kellar et al., 1976; Yagi et al., 1977a; Yang et al., 1977; Whalen et al., 1979). Consistent with this property is the finding that nucleophilic substitution by DNA bases occurs at this site (Weinstein et al., 1976; Straub et al., 1977; Wood et al., 1977); we expect RNA to form the same type of adducts. Initial cleavage of the bond between C-10 of the hydrocarbon and the alkylation site on the base results in a hydrocarbon fragment (BPT^+) at m/z 345. Loss of methanol then gives m/z 313; further loss of methanol or methoxy radical gives m/z 281 or 282. Successive loss from the latter ion of methyl radical and CO gives m/z 267 and 239. The ion at m/z 281 occurs at high intensity in spectra from all samples; ions at m/z 282, 267, and 239 occur at moderate intensities.

The $[BPT{\cdot}N(CH_3)]^+$ fragment is generated by cleavage of the bond between the exocyclic amino group of the base (which bears a methyl group due to the permethylation) and the adjacent ring carbon of the base. Because the heterocyclic bases do not undergo significant fragmentation (von Minden & McCloskey, 1973), this is the only reasonable mechanism for the occurrence of this ion. $[BPT{\cdot}N(CH_3)]^+$ was not observed directly, but ions observed at m/z 344, 341, 313, 295, 269, and 255 are consistent with some of its expected fragments. Table VI lists these fragments as well as possible fragments with the same masses from BPT^+ or tetrol.

Tetrol in these samples could arise from adduct degradation. We have found that, during storage at 4 °C in the dark, BPDE adducts decompose at a rate of a few percent a month, producing tetrol; the rate of decomposition is accelerated by light (Geacintov et al., 1987). (Tetrol from the hydrolysis of BPDE during the RNA modification reaction would be removed by the adduct isolation procedure.) The ions at m/z 344, 313, 269, and 255 could be produced from tetrol or BPT^+.

Since the peaks at m/z 341 and 295 can arise from $[BPT{\cdot}N(CH_3)]^+$ but not from BPT^+ or tetrol, they are indicative of alkylation at the exocyclic amine. Each of our samples produced these ions, indicating that the exocyclic amine is the BPDE alkylation target of the major Guo, Ado, or Cyd adduct in the peaks analyzed. Similar reasoning was previously used to identify the BPDE alkylation sites in dGuo and dAdo adducts from DNA (Straub et al., 1977). However, due to the low levels of alkylation, insufficient dCyd adduct was recovered to permit complete structural analysis.

Chart I: Major Structures Identified in the Permethylated Guo (1), Ado (2), and Cyd (3) Adducts from (±)-*anti*-BPDE-Modified RNA

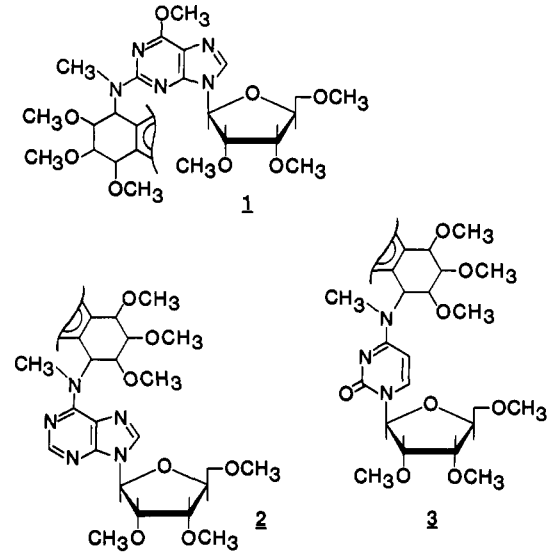

Conclusion

The identity of the base in the major alkali-stable adducts formed by reaction of (±)-*anti*-BPDE and yeast RNA has been determined by comparison of HPLC retention times (see Figure 2) with those of BPDE adducts from poly(G), poly(A), and poly(C), and by EI and liquid SI mass spectrometry. While BPDE adducts formed with poly(G) and poly(C) coelute with peak 1, the mass spectra of the peak 1 fraction indicate only the presence of a Guo adduct. The presence of a Cyd adduct in peak 2 is confirmed by EIMS. In the case of peak 4, all techniques show that a Cyd adduct is present, but LSIMS also reveals the presence of a Guo adduct, probably due to overlap with peak 3. EIMS and HPLC retention times are consistent with the presence of both Ado and Cyd adducts in peak 6. In the remaining peaks all three techniques agree.

The three principal structures that have been identified among the BPDE–RNA adducts are illustrated in Chart I. These structures are analogous to those of known or suspected DNA adducts. The multiple adducts involving the same exocyclic amine alkylation site that form with each base are probably diastereomers resulting from the presence of two enantiomers of *anti*-BPDE (Meehan & Straub, 1978) with cis and trans opening of the epoxide ring (Weinstein et al., 1976).

ACKNOWLEDGMENTS

We thank Dr. George Shimer for review of the manuscript and Andrea Mazel and Gloria de la Cruz for its preparation. LSIMS was carried out at the Bioorganic and Biomedical Mass Spectrometry Resource of the University of California at San Francisco. EIMS was performed at the Michigan State University Mass Spectrometry Facility (Department of Biochemistry). We are grateful to Brian Musselman (of the latter facility) for advice on the permethylation procedure.

SUPPLEMENTARY MATERIAL AVAILABLE

Electron-impact mass spectra of the BPDE–Guo adduct (Figure 1), BPDE–Ado adduct (Figure 2), BPDE–Cyd adduct (Figure 3), and BPDE–Guo plus BPDE–Cyd adducts (Figure 4) from peaks 1, 8, 2, and 4, respectively (4 pages). Ordering information is given on any current masthead page.

REFERENCES

Brookes, P., & Lawley, P. D. (1964) *Nature (London) 202*, 781–784.

Buening M. K., Wislocki, P. G., Levin, W., Yagi, H., Thakker, D. R., Akagi, H., Koreeda, M., Jerina, D. M., & Conney, A. H. (1978) *Proc. Natl. Acad. Sci. U.S.A. 75*, 5358–5361.

Constant, J. F., Laûgaa, P., Roques, B. P., & Lhomme, J. (1988) *Biochemistry 27*, 3997–4003.

Geacintov, N. E., Prusik, T., & Khosrofian, J. M. (1976) *J. Am. Chem. Soc. 98*, 6444–6452.

Geacintov, N. E., Hibshoosh, H., Ibanez, V., Benjamin, M. J., & Harvey, R. G. (1984) *Biophys. Chem. 20*, 121–133.

Geacintov, N. E., Zinger, D., Ibanez, V., Santella, R., Grunberger, D., & Harvey, R. G. (1987) *Carcinogenesis (London) 8*, 925–935.

Gelboin, H. V. (1969) *Cancer Res. 29*, 1272–1276.

Hakamori, S.-I. (1964) *J. Biochem. (Tokyo) 55*, 205–208.

Harvey, R. G., & Fu, P. P. (1978) in *Polycyclic Hydrocarbons and Cancer* (Gelboin, H. V., & T'so, P. O. P., Eds.) Vol. 1, pp 133–165, Academic Press, New York.

Heidelberger, C. (1975) *Annu. Rev. Biochem. 44*, 79–121.

Huberman, E., Sacks, L., Yang, S. K., & Gelboin, H. V. (1976) *Proc. Natl. Acad. Sci. U.S.A. 73*, 607–611.

Ivanovic, V., Geacintov, N. E., Yamasaki, H., & Weinstein, I. B. (1978) *Biochemistry 17*, 1597–1603.

Jeffrey, A. M., Jennette, K. W., Blobstein, S. H., Weinstein, I. B., Beland, F. A., Harvey, R. G., Kasai, H., Miura, I., & Nakanishi, K. (1976) *J. Am. Chem. Soc. 98*, 5714–5715.

Jeffrey, A. M., Grzeskowiak, K., Weinstein, I. B., Nakanishi, K., Roller, P., & Harvey, R. G. (1979) *Science 206*, 1309–1311.

Kellar, J. W., Heidelberger, C., Beland, F. A., & Harvey, R. G. (1976) *J. Am. Chem. Soc. 98*, 8276–8277.

King, H. W. S., Osborne, M. R., Beland, F. A., Harvey, R. G., & Brookes, P. (1976) *Proc. Natl. Acad. Sci. U.S.A. 73*, 2679–2681.

Koreeda, M., Moore, P. D., Yagi, H., Yeh, H. J., & Jerina, D. M. (1976) *J. Am. Chem. Soc. 98*, 6720–6722.

McCann, J., & Ames, B. N. (1976) *Proc. Natl. Acad. Sci. U.S.A., 73*, 950–954.

Meehan, T., & Straub, K. (1979) *Nature (London) 277*, 410–412.

Meehan, T., Straub, K., & Calvin, M. (1976) *Proc. Natl. Acad. Sci. U.S.A. 73*, 1437–1441.

Meehan, T., Straub, K., & Calvin, M. (1977) *Nature (London) 269*, 725–727.

Miller, E. C., & Miller, J. A. (1971) in *Chemical Mutagens* (Hollaender, A., Ed.) Vol. 1, pp 83–119, Plenum, New York.

Nakanishi, K., Kasai, H., Cho, H., Harvey, R. G., Jeffrey, A. M., Jennette, K. W., & Weinstein, I. B. (1977) *J. Am. Chem. Soc. 99*, 258–260.

Osborne, M. R., Harvey, R. G., & Brookes, P. (1978) *Chem.-Biol. Interact. 20*, 123–130.

Osborne, M. R., Jacobs, S., Harvey, R. G., & Brookes, P. (1981) *Carcinogenesis (London) 2*, 553–558.

Panthananickal, A., & Marnett, L. J. (1981) *J. Chromatogr. 206*, 253–265.

Sims, P., Grover, P. L., Swaisland, A., Pal, K., & Hewer, A. (1974) *Nature (London) 252*, 326–328.

Sjöberg, K. (1966) *Tetrahedron Lett. 51*, 6383–6384.

Straub, K., Meehan, T., Burlingame, A. L., & Calvin, M. (1977) *Proc. Natl. Acad. Sci. U.S.A. 74*, 5285–5289.

von Minden, D. L., & McCloskey, J. A. (1973) *J. Am. Chem. Soc. 95*, 7480–7490.

Weinstein, I. B., Jeffrey, A. M., Jennette, K. W., Blobstein, S. F., Harvey, R. G., Harris, C., Autrup, H., Kasai, H., & Nakanishi, K. (1976) *Science 193*, 592–595.

Whalen, D. L., Ross, A. M., Montemarano, J. A., Thakker, D. R., Yagi, H., & Jerina, D. M. (1979) *J. Am. Chem. Soc. 101*, 5086–5088.

Wood, A. W., Chang, R. L., Levin, W., Yagi, H., Thakker, D. R., Jerina, D. M., & Conney, A. H. (1977) *Biochem. Biophys. Res. Commun. 77*, 1389–1396.

Yagi, H., Thakker, D. R., Hernandez, O., Koreeda, M., & Jerina, D. M. (1977a) *J. Am. Chem. Soc. 99*, 1604–1611.

Yagi, H., Akagi, H., Thakker, D. R., Mah, H. D., Koreeda, M., & Jerina, D. M. (1977b) *J. Am. Chem. Soc. 99*, 2358–2359.

Yang, S. K., McCourt, D. W., & Gelboin, H. V. (1977) *J. Am. Chem. Soc. 99*, 5130–5134.